

# Determination of Phase Transformation and Activation Energy in High Temperature Shape Memory Ti-V-Al Alloy

Semra Ergen 

Gaziosmanpasa University, Department of Physics, Tokat, Turkey.

## ABSTRACT

Ti-V-Al alloys are a good candidates for lightweight high temperature shape memory alloys. Due to their excellent mechanical properties with low density, in industrial applications, there are widely used as high temperature shape memory alloys. However, Ti-V-Al alloys have cold workability. Because of this feature, machinability in different forms is quite easy and cheap. In this work, microstructure and phase transformation of Ti-V-Al alloy produced by arc-melting method were investigated. The phase formations, microstructures, martensite-austenite transformation temperatures were characterized using XRD, SEM and DSC. Activation energies of the alloy were calculated by Kissinger and Osawa methods.

### Keywords:

High Temperature, Shape memory alloys, Phase transformations, Martensitic transformation, Activation energy

## INTRODUCTION

High temperature shape memory alloys (HTSMA) with are potentially engineered to operate at temperatures above 100 ° C in the automotive, aerospace, and manufacturing industries. The HTSMA can be categorized into three groups depending on the transformation temperatures. First group; 100-400 ° C, the second group is 400-700 ° C and the third group is alloys having temperatures above 700 ° C [1].

There are many high temperature shape memory alloys in the literature. Some of these are Ni-Ti-X (X = Pt, Pd, Hf, Zr), Ni-Al, Cu-Al-Ni, Ni-Mn-Ga and Ti-Ta alloys [2-4]. These alloys have many problems that limit their practical application. The Ni-Ti-Pd / Pt alloy is quite expensive due to the Pd / Pt content. Ni-Ti-Hf / Zr alloys have poor cold workability [1]. Ni-Mn-Ga alloys are cracked at relatively high temperatures [5]. Ni-Al alloy is virtually no plastic at room temperature [1]. Cu-Al-Ni alloys have brittle phase deposits that cause poor ductility at grain boundaries of 1 mm size and large grains [6]. However, the density of all these high temperature shape memory alloys is still relatively high (6,4 -9 gr/cm<sup>3</sup>). The high density of these alloys does not meet the demand for weight reduction in aerospace applications [7]. For this reason, it is necessary to produce and develop lighter high temperature shape

memory alloys.

Ti-V-Al alloys are a good candidate for lightweight high temperature shape memory alloys. First, the densities of Ti-V-Al alloys are very low and close to the density of nearly pure titanium (4, 5 g / cm<sup>3</sup>). However, Ti-V-Al alloys have excellent cold workability, which can be reduced by more than 90% [8].

As mentioned above, Ti alloys used in many areas are preferred, especially in aircraft engines compared to other alloys in the aerospace industry due to their high temperature properties as well as their lightness, high strength (high specific strength) and heat resistance properties. Turbo fan motors used on aircrafts; Propeller, compressor, ignition chamber and tribune. Ti alloys are generally used in propeller and compressor sections located at the front of the engine where the air temperature is relatively low (400 ° C and lower). At the back of the aircraft, the tribune and combustion chamber parts use alloys with higher temperatures (700 ° C and higher). Ti alloys are also used in these parts of the aircraft, in the propeller and compressor sections, which are located in the front section of the engine where the temperature is relatively low (400 ° C and lower). Alloys with higher temperatures (700 ° C and higher) are used in the tribune and combustion

### Article History:

Received: 2017/06/08

Accepted: 2017/09/10

Online: 2017/12/22

### Correspondence to: Semra Ergen

Gaziosmanpasa University, Faculty of Science and Arts, Department of Physics Tokat, Turkey

Tel: +90 (356) 252-1616

Fax: +90 (356) 252 1585

E-Mail: semraergengap@gmail.com

chamber parts in the back half of the aircraft.

In the present study, Ti-15V-4Al alloy was produced by arc melting technique to be used in the front panels of aircraft engines in the aviation industry. Phase structures, microstructures and transformation temperatures of alloy were characterized with XRD, SEM and DSC techniques. Solid phase transformation properties of alloy were investigated by DSC technique at various heating/cooling rates. In the investigations made, it was observed how the phase transformation temperatures and the activation energy change with the heating/cooling rate and the number of thermal cycles. It has been generally determined that the phase transformation temperatures and the activation energy values reduce by the increase in the heating/cooling rate and their did not changed with the number of cycles. Thermal activation energy can be defined as the energy required during phase transformation of materials [9]. The calculation method of this energy was previously acquired by Kissinger and Ozawa [10,11]. The phase transformation temperatures are based on the fact that the material changes with the heating rate. At least four different heating and cooling rates were used in the calculation of the activation energy of the alloy. The energy values obtained by both Kissinger and Osawa methods were close to each other. It is seen that the activation energy values of alloy is much lower when compared to Ni-Ti. This means that activating the solid-solid transformation of the alloy is much easier than with the Ni-Ti alloy, which is an advantage for the Ti-V-Al alloy. In this manner, Ti-V-Al alloy which could be an alternative to the Ni-Ti alloy, was produced which was both lighter and more active.

## EXPERIMENTAL

Ti-15V-4Al (wt %) alloy was prepared by vacuum arc melting in a water-cooled copper crucible under an Ar atmosphere using high purity Ti, V and Al. During the melting, zirconium was used as a getter material to reduce oxygen contamination of the prepared alloy

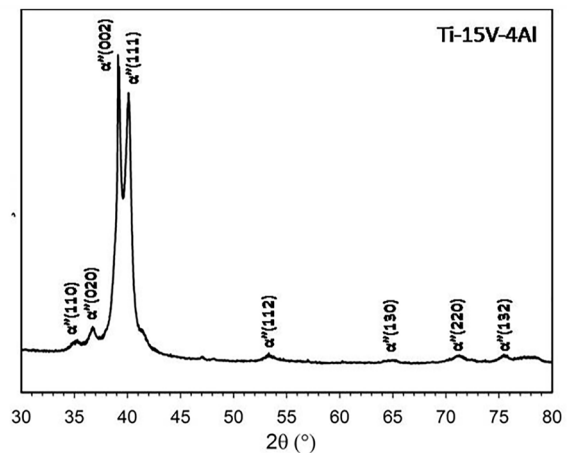


Figure 1. The X-ray diffraction pattern of Ti-15V-4Al alloy.

buttons. The Ti-15V-4Al alloy was remelted many times for homogenization and was homogenized at 950 °C for 8 h in vacuum-sealed quartz tubes. And then was quenched in ice water by breaking the tubes. The transformation temperatures of the alloy were examined by differential scanning calorimetry. The differential scanning calorimetry measurements were carried out by a DSC 131 equipment (Setaram, France) at different heating/cooling rates in the temperature range 25–500 °C. The surface of the TiVAl alloy etched with 10ml HF+ 20ml HNO<sub>3</sub> + 40ml H<sub>2</sub>O solution for SEM analysis. The alloy was thermally cycled three times in the DSC to determine the stability of the transformation peaks. Activation energy of alloy has been determined by Kissinger and Osawa methods.

## RESULTS AND DISCUSSION

Figure 1 shows the X-ray diffraction pattern of Ti-15V-4Al alloy at room temperature. It was understood that when the diffraction peaks were indicated, the alloy contained entirely orthorhombic α'' martensite phase. This indicates that the martensitic transformation temperature is above room temperature and the microstructure of the alloy is entirely composed of the α'' martensite phase.

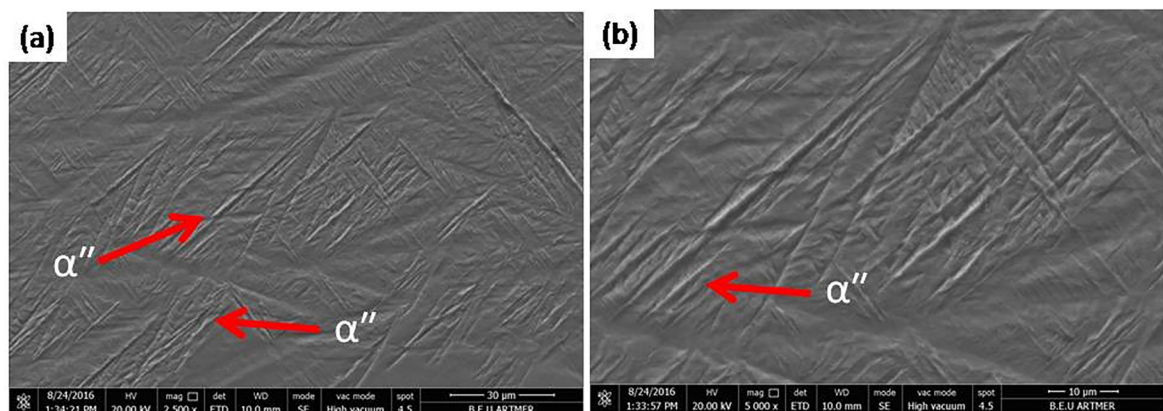


Figure 2. The SEM photographs of Ti-15V-4Al alloy.

**Table 1.** The starting and finishing temperatures (As, Af) of the reverse martensitic transformation, the enthalpy and activation energy values.

Heating Rate (°C/min)	As (°C)	Af (°C)	$\Delta H_{MA}$ (kJ/mol)	$E_{Kissinger}$ (kJ/mol)	$E_{Osawa}$ (kJ/mol)
5	150	230	42	13.71	11.14
10	200	271			
15	210	297			
20	211	300			

**Table 2.** Reverse martensitic transformation temperatures under thermal cycling depending on heating-cooling rate.

Heating Rate (°C/dk)	Cycle Number	As (°C)	Af (°C)
10	1	209	298
	2	212	301
	3	218	308
20	1	211	312
	2	218	314
	3	219	318

Figure 2 shows the SEM photographs taken at 2500 and 5000 magnifications of the alloy. The microstructure of alloy consists entirely of  $\alpha''$  martensite phases. The martensite structures which are formed in a acicular shape are indicated by arrows in the Figure 2. As can be seen, SEM analyzes are consistent with XRD results.

Figure 3 shows the DSC curves recorded at four different heating cooling rates of Ti-15V-4Al alloy. The alloy exhibits a typical stepwise thermoelastic martensitic transformation (MT). In the DSC, the endothermic peak on the heating curves shows the reverse martensitic transformation from orthorhombic martensite to cubic

austenite. The reverse martensitic transformation temperatures were measured by tangent method according to the DSC curves. An endothermic peak showing reverse martensitic transformation temperatures on the heating is clearly visible starting (As) temperature of 211 ° C and finish (Af) temperature of 300 ° C at heating and cooling rate of 20 °C/min. However, no significant exothermic peaks were detected on cooling. This phenomenon is similar to that of Ti-20Zr-10Nb [12], Ti-19Nb-9Zr [13] and Ti-30Ta [14] alloys, which can be attributed to the low enthalpy of transformation from  $\beta$  to  $\alpha''$  or the partial transformation from  $\beta$  phase to  $\alpha''$  martensite phase. This makes the martensite transformation peak too small to be detected by the DSC [12,15]. The starting and finishing temperatures (As, Ap, Af) of the reverse MT and the enthalpies depending on heating-cooling rate are summarized in Table 1.

In Fig. 3 (a-d), reverse martensitic transformation peaks are observed for heating cooling rates of 5, 10, 15 and 20 °C/min, respectively.

The transformation temperature graph versus heating rate is plotted in Figure 4. A small increase in transformation temperatures was observed as the heating rate increased. The reason for this increase is thought to be due to the internal friction in the microstructure [16].

In the Figure 5 (a,b), the DSC graphs belonging to the cycle analyses at heating and cooling rate of 10 °C/min and 20 °C/min are given for Ti-15V-4Al alloy.

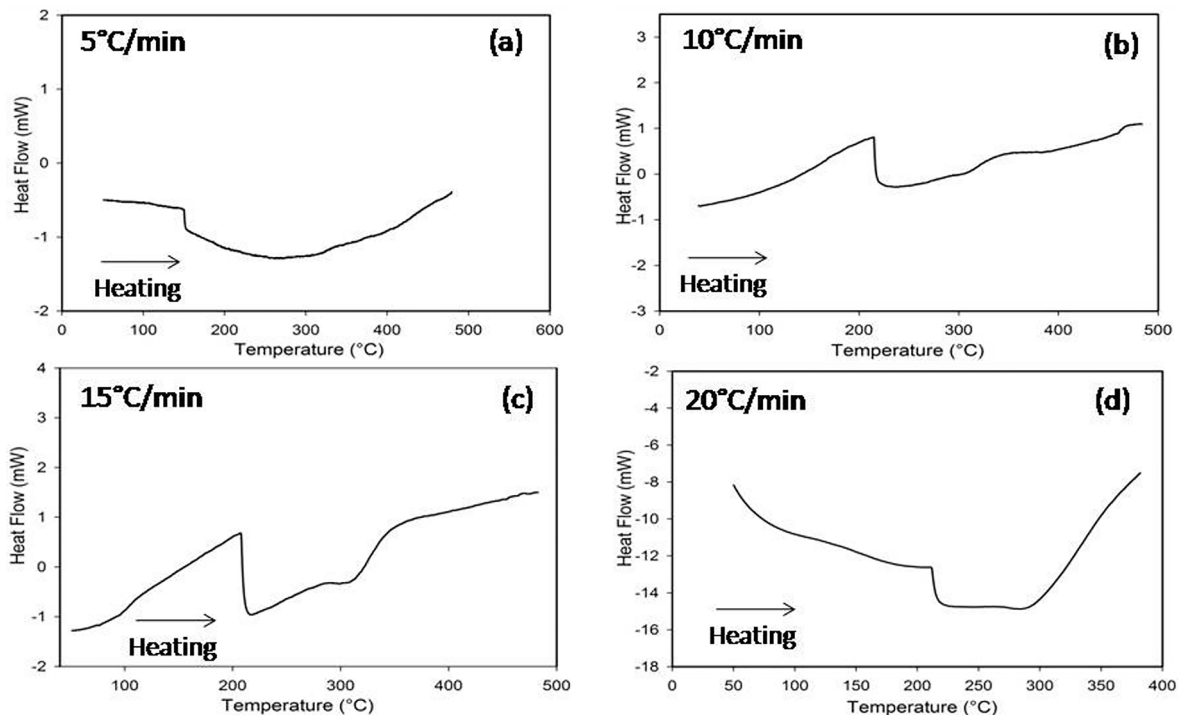


**Figure 3.** The DSC curves taken at four different heating-cooling rates of Ti-15V-4Al alloy. a) 5°C/min b) 10°C/min c) 15°C/min d) 20°C/min

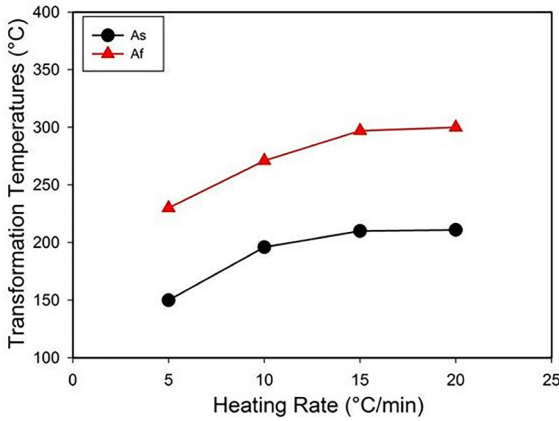


**Fig 4.** The transformation temperatures depending on heating-cooling rate of Ti-15V-4Al alloy.

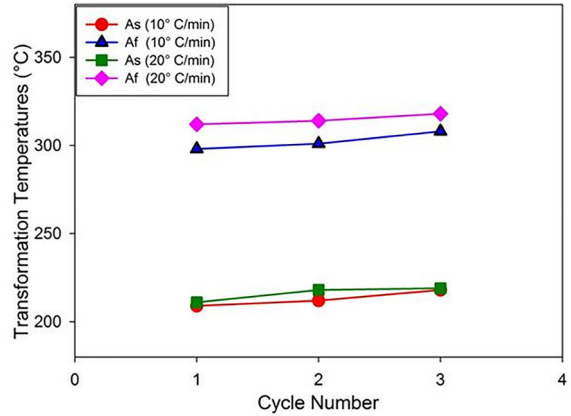


**Fig 6.** The reverse martensitic transformation temperatures depending on the number of cycles.

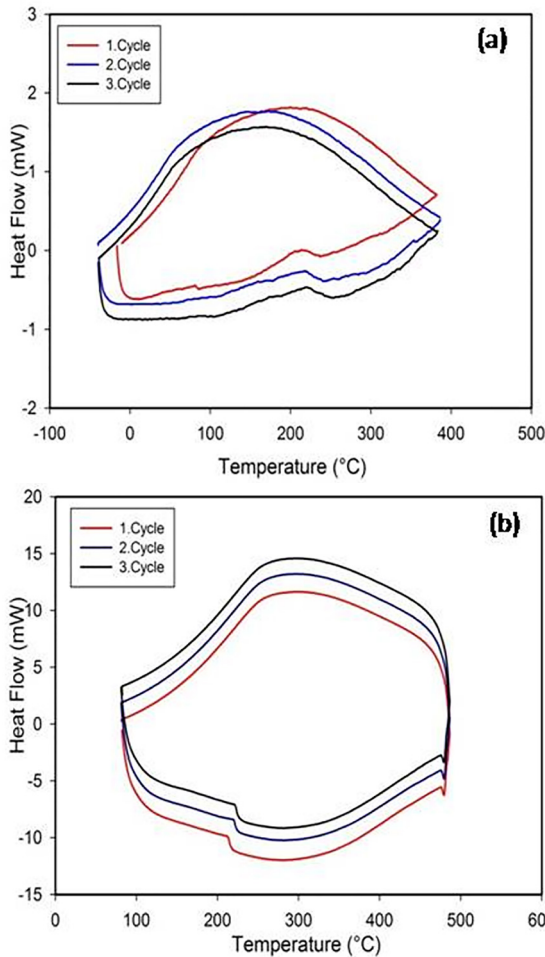


**Fig 5.** The thermal cycling analyses of Ti-15V-4Al alloy at heating-cooling rate a) 10 °C/min and b) 20°C/min

Figure 6 shows how the reverse martensitic transformation temperature changes with the number of cycles. No significant change in transformation temperatures was observed as the number of cycles increased at two different heating and cooling rates (Table 2). This means that the reverse martensitic transformation

is stable. It is necessary to interpret it together with the TEM analysis in order to investigate both the number of cycles and the changes depending on the heating rate in more detail.

The energy that the material needs for phase transformation is called the activation energy. This energy can be found by making use of thermal cycling curves made with different heating rates [10-11]. Kissinger ve Osawa methods are available for estimating the kinetic parameters of materials from the DSC results. The Kissinger and Osawa methods for estimating the activation energy,  $E_A$  is derived from the following equation based on the maximum rate of phase transformation occurring at temperature  $T_m$ . According to the Kissinger method, the formula in equation 2 is used, and according to Osawa method, the formula in equation 3 is used in the calculation of activation energies.

$$\frac{d\alpha}{dT} = \frac{A}{\beta} \exp\left(\frac{E_A}{RT}\right)(1-\alpha)^n \quad (1)$$

For Kissinger method, by plotting  $\ln\left(\frac{\beta}{T_m^2}\right)$  versus  $\ln\left(\frac{1000}{T_m}\right)$ , the slope of the plot equals  $-\frac{E_A}{R}$  and subsequently the value of  $E_A$  can be obtained.

$$\frac{d\left(\ln\left(\frac{\beta}{T_m^2}\right)\right)}{d\left(\ln\left(\frac{1000}{T_m}\right)\right)} = -\frac{E_A}{R} \quad (2)$$

As for Osawa method, by plotting  $\ln(\beta)$  versus  $\ln\left(\frac{1000}{T_m}\right)$ , with multiplying the slope of the plot equation by 2.19, the value of  $E_A$  can be obtained.

$$\frac{d(\ln(\beta))}{d\left(\ln\left(\frac{1000}{T_m}\right)\right)} = 2.19 \times -\frac{E_A}{R} \quad (3)$$

In these equations, R is the general gas constant ( $R = 8,314 \text{ J / mol}$ ),  $E_A$  is the activation energy,  $\beta$  is the heating rate, and  $T_m$  is the temperature corresponding to the

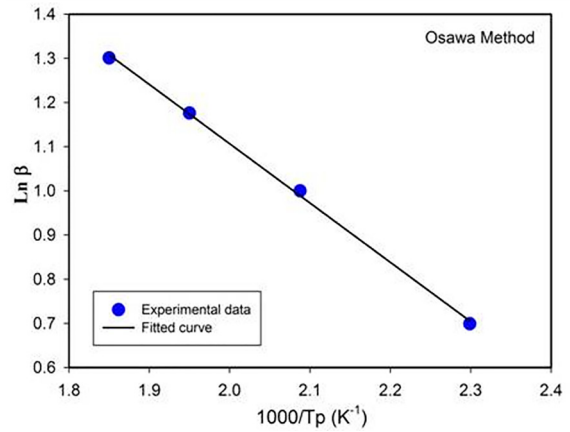
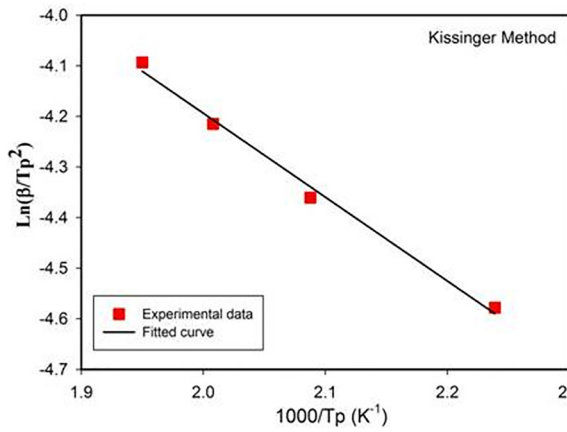


Fig 7. Determination of  $E_A$  for Ti-15V-4Al alloy using a) Kissinger and b) Osawa methods.

maximum peak during transformation in the DSC curve. The Kissinger and Osawa methods to estimate the kinetic parameters requires the DSC results obtained under at least three heating rates (Fig. 7).

The calculated activation energy values were 13.71 kJ / mol according to the Kissinger method and 11.14 kJ / mol according to the Osawa method. The activation energies calculated by both methods are found to be close to each other (Table 1). It is seen that these values are much lower when compared to the activation energy value of the Ni-Ti alloy. This means that activating Ti-V-Al alloy is easier than Ni-Ti alloy [17].

## CONCLUSIONS

In this study, phase transformation and microstructure of Ti-15V-4Al alloy were investigated by XRD and SEM analysis. Reverse transformation temperatures and phase transformation properties were examined by DSC technique as a function of heating-cooling rate and number of cycles. The results are summarized below.

1. The results show that the Ti-15V-4Al alloy is composed of a single orthorhombic  $\alpha''$ -martensite phase at room temperature.
2. It was observed that the microstructure of the alloy contained martensite structures with a spindle-like shape.
3. The  $A_s$  and  $A_f$  reverse martensitic transformation temperatures were approximately found to be 211 and 300 °C at heating-cooling rate of 20°C/min, respectively. No obvious exothermic peak was detected for Ti-15V-4Al alloy during cooling from 500 °C to room temperature.
4. From the DSC analyses, it was found that the increase in the heating rate caused a small increase in the reverse martensitic transformation temperatures.
5. No significant change in the reverse transformation

temperatures of the alloy was observed as the number of cycles increased from the thermal cycling analyzes.

6. It was observed that the activation energy values calculated by both methods are close to each other and much lower than the energy values of the Ni-Ti alloy.

## REFERENCES

1. Ma, J., Karaman, I., and Noebe, R.D. High temperature shape memory alloys. *International Materials Reviews* 55: 5 (2010) 257-315.
2. Atli, K.C., Karaman, I., Noebe, R.D., Garg, A., Chulyakov, Y.I., Kireeva, I.V. Shape memory characteristics of  $Ti_{49.5}Ni_{25}Pd_{25}Sc_{0.5}$  high-temperature shape memory alloy after severe plastic deformation. *Acta Mater* 59 (2011) 4747-4760.
3. Meng, X.L., Cai, W., Wang, L.M., Zheng, Y.F., Zhao, L.C., Zhou, L.M. Microstructure of stress-induced martensite in a Ti-Ni-Hf high temperature shape memory alloy. *Scripta Mater* 45 (2001) 1177-1182.
4. Zheng, X.H., Sui, J.H., Zhang, X., Yang, Z.Y., Wang, H.B., Tian, X.H., Cai, W. Thermal stability and high-temperature shape memory effect of Ti-Ta-Zr alloy. *Scripta Mater* 68 (2013) 1008-1011.
5. Ma, Y., Yang, S., Liu, Y., Liu, X. The ductility and shape-memory properties of Ni- Mn-Co-Ga high-temperature shape-memory alloys. *Acta Mater* 57 (2009) 3232-3241.
6. Kato, H., Stalmans, R., Van Humbeeck, J. Two-way shape memory effect induced by tension training in Cu-13.4Al-4.0Ni (mass%) alloy single crystals. *Mater. Trans.* 39 (1998) 378-386.
7. Yang, Z.Y., Zheng, X.H., Wu, Y., Cai, W. Martensitic transformation and shape memory behavior of Ti-V-Al-Fe lightweight shape memory alloys. *Journal of Alloys and Compound*, 680 (2016) 462-466.
8. Yang, Z.Y., Zheng, X.H., Cai, W. Martensitic transformation and shape memory effect of Ti-V-Al lightweight high-temperature shape memory alloys. *Scripta Materialia* 99 (2015) 97-100
9. Kok M., Yakinci ZD., Aydogdu A., Aydogdu Y. Thermal and magnetic properties of Ni51Mn28.5Ga19.5B magnetic-shape-memory alloy. *J Therm Anal Calorim* 115 (2014)

- 555–559.
10. Kissinger, H. E. Reaction Kinetics in Differential Thermal Analysis. Analytical Chemistry. 29 No. 11, National Bureau of Standards, Washington, pp. 1702–1706, 1957.
  11. Ozawa, T. A new method of analyzing thermogravimetric data. *Chem. Soc. Jpn* 38 (11) (1965) 1881–1886.
  12. Cui, Y., Li Y., Luo K., Xu H. Microstructure and shape memory effect of Ti-20Zr-10Nb alloy. *Mat. Sci. Eng. A*. 527 (2010) 652–656.
  13. Ma, L.W., Cheng, H.S., Chung, C.Y., Yuan, B. Effect of heat treatment time on microstructure and mechanical properties of Ti-19Nb-9Zr (at%) shape memory alloy. *Materials Science & Engineering A* 561 (2013) 427-433.
  14. Zheng XH, Sui JH, Zhang X, Tian XH, Cai W. Effect of Y addition on the martensitic transformation and shape memory effect of Ti-Ta high-temperature shape memory alloy. *Journal of Alloys and Compounds* 539 (2012) 144–147.
  15. Takahashi, E., Sakurai, T., Watanabe, S., Masahashi, N., Hanada, S. Effect of heat treatment and Sn content on superelasticity in biocompatible TiNbSn alloy. *Mater. Trans.* 43 (12) (2002) 2978-2983.
  16. Acar E. Dynamic mechanical response of a Ni45.7Ti29.3Hf20Pd5 alloy. *Materials Science and Engineering :A* (2015) 633 169–175.
  17. Fang, H., Wong, B., Bai, Y. Kinetic modeling of thermophysical properties of shape memory alloys during phase transformation. *Construction and Building Materials* 131 (2017) 146–155.